# Potentiometric and Further Kinetic Characterization of the Flavin-Binding Domain of *Saccharomyces cerevisiae* Flavocytochrome $b_2$. Inhibition by Anions Binding in the Active Site†

Narimantas Čénas,‡ K. H. Diêp Lê,§ Micheline Terrier,§ and Florence Lederer*,§

*CNRS FRE2930, Laboratoire d'Enzymologie et Biochimie Structurales, CNRS, Avenue de la Terrasse, 91198 Gif-sur-Yvette Cedex, France, and Institute of Biochemistry, Mokslininku 12, Vilnius 2600, Lithuania*

*Received December 22, 2006; Revised Manuscript Received February 7, 2007*

ABSTRACT: *Saccharomyces cerevisiae* flavocytochrome $b_2$ (L-lactate:cytochrome *c* oxido reductase, EC 1.1.2.3) is a homotetramer, with FMN and protoheme IX binding on separate domains. The flavin-binding domains form the enzyme tetrameric core, while the cytochrome $b_2$ domains appear to be mobile around a hinge region (Xia, Z. X., and Mathews, F. S. (1990) *J. Mol. Biol. 212*, 867−863). The enzyme catalyzes electron transfer from L-lactate to cytochrome *c*, or to nonphysiological acceptors such as ferricyanide, via FMN and heme $b_2$. The kinetics of this multistep reaction are complex. In order to clarify some of its aspects, the tetrameric FMN-binding domain (FDH domain) has been independently expressed in *Escherichia coli* (Balme, A., Brunt, C. E., Pallister, R., Chapman, S. K., and Reid, G. A. (1995) *Biochem. J. 309*, 601−605). We present here an additional characterization of this domain. In our hands, it has essentially the same ferricyanide reductase activity as the holo-enzyme. The comparison of the steady-state kinetics with ferricyanide as acceptor and of the pre-steady-state kinetics of flavin reduction, as well as the kinetic isotope effects of the reactions using L-2-[$^2$H]lactate, indicates that flavin reduction is the limiting step in lactate oxidation. During the oxidation of the reduced FDH domain by ferricyanide, the oxidation of the semiquinone is much faster than the oxidation of two-electron-reduced flavin. This order of reactivity is reversed during flavin to heme $b_2$ transfer in the holo-enzyme. Potentiometric studies of the protein yielded a standard redox potential for FMN at pH 7.0, $E°_7$, of −81 mV, a value practically identical to the published value of −90 mV for FMN in holo-flavocytochrome $b_2$. However, as expected from the kinetics of the oxidative half-reaction, the FDH domain was characterized by a significantly destabilized flavin semiquinone state compared with holo-enzyme, with a semiquinone formation constant *K* of 1.25−0.64 vs 33.5, respectively (Tegoni, M., Silvestrini, M. C., Guigliarelli, B., Asso, M., and Bertrand, P. (1998) *Biochemistry, 37*, 12761−12771). As in the holo-enzyme, the semiquinone state in the FDH domain is significantly stabilized by the reaction product, pyruvate. We also studied the inhibition exerted in the steady and pre steady states by the reaction product pyruvate and by anions (bromide, chloride, phosphate, acetate), with respect to both flavin reduction and reoxidation. The results indicate that these compounds bind to the oxidized and the two-electron-reduced forms of the FDH domain, and that excess L-lactate also binds to the two-electron-reduced form. These findings point to the existence of a common or strongly overlapping binding site. A comparison of the effect of the anions on WT and R289K holo-flavocytochromes $b_2$ indicates that invariant R289 belongs to this site. According to literature data, it must also be present in other members of the family of L-2-hydroxy acid-oxidizing enzymes.

Flavocytochrome $b_2$ (Fcb2[1]) from *Sacharomyces cerevisiae* (L-lactate: cytochrome *c* oxido reductase, EC 1.1.2.3) is a component of yeast mitochondrial intermembrane space (*1*), where it catalyzes the oxidation of L-lactate to pyruvate and transfers the reducing equivalents to cytochrome *c* (*2*). The enzyme is a homotetramer (4 × 57 kDa) (*3*), with each subunit composed of two functionally distinct domains, a C-terminal flavodehydrogenase (FDH) domain containing FMN and an N-terminal cytochrome domain with protoheme IX (*4*). The crystal structure indicates that the heme domain is mobile with respect to the tetrameric flavodehydrogenase core.

The steady- and pre-steady-state kinetics of Fcb2 under a variety of conditions (*5*−*8*), as well as the redox potentials of its prosthetic groups (*5*, *9*, *10*), and the mechanism of electron transfer to cytochrome *c* (*11*−*14*) have been the focus of numerous studies. The enzyme catalytic cycle involves the oxidation of lactate to pyruvate with FMN

† This work was supported by the European Union (Human Capital and Mobility Program, Network FLAPS) and by fellowships to N.Č. from the CNRS and the Ministère de l'Enseignement Supérieur.

* To whom correspondence should be addressed: CNRS FRE2930, Laboratoire d'Enzymologie et Biochimie Structurales, CNRS, Avenue de la Terrasse, 91198 Gif-sur-Yvette Cedex, France. Tel: 33 1 69 82 34 64. Fax: 33 1 69 82 31 29. E-mail: lederer@lebs.cnrs-gif.fr.

‡ Institute of Biochemistry.

§ Laboratoire d'Enzymologie et Biochimie Structurales, CNRS.

[1] Abbreviations: Fcb2, flavocytochrome $b_2$; FDH, flavodehydrogenase; $Fl_{ox}$, oxidized flavin or FMN; $Fl_{sq}$, flavin semiquinone or $FMN^{-}\cdot$; $Fl_{red}$, reduced flavin or $FMNH^{-}$; nNOS, neuronal nitric-oxide synthase.

10.1021/bi602634y CCC: $37.00 
Published on Web 03/21/2007

Scheme 1

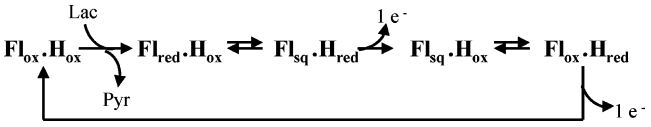


reduction as the main rate-limiting step (*8*, *15*), then two subsequent single-electron transfers from reduced FMN and its anionic semiquinone to heme $b_2$, with a net reduction of two cytochrome *c* molecules (*5*, *11*−*13*) (Scheme 1). The enzyme crystal structure shows that the relevant flavin to heme electron transfers must take place within a subunit, with a shortest edge to edge distance between prosthetic groups of 0.96 nm (*4*). When ferricyanide is used as acceptor, it is considered that it takes electrons from the reduced heme as well as from the flavin semiquinone (*16*).

Flavocytochrome $b_2$ is known to be inhibited by oxalate (*17*−*20*), by the reaction product pyruvate (*6*, *9*, *14*, *18*, *19*) and high acetate concentrations (*21*). As a rule, in the steady state, the above compounds act as noncompetitive and/or mixed inhibitors toward the substrate L-lactate. This was ascribed to their binding to several enzyme redox states. It was shown in particular that pyruvate binds at the active site with different affinities depending on the flavin redox state; pyruvate binding to the semiquinone state increases the redox potential and inhibits electron transfer to heme $b_2$ (*9*, *10*, *22*). Interestingly, Fcb2 is also inhibited by excess L-lactate (*3*, *19*, *21*).

In order to dissect the enzyme properties, several approaches were devised in the past to study the FDH domain independently from the heme domain. A heme-free preparation was obtained from the Fcb2 apoprotein by reconstitution with FMN (*16*); in addition, the two domains of the *Hansenula anomala* enzyme were separated by mild proteolysis (*23*); more recently, the recombinant tetrameric FDH domain of *S. cerevisiae* Fcb2 was expressed separately in *Escherichia coli* (*24*). Its crystal structure at 2.50 Å resolution showed little overall difference with that in the intact enzyme (*25*). The few kinetic studies of these FDH domain preparations showed that the kinetic parameters for the reductive half-reaction were rather similar to those of the intact enzyme but that the tetrameric domain was unable to efficiently reduce cytochrome *c* (*16*, *23*, *24*, *26*). Moreover, the pre-steady-state reoxidation of the heme-free Fcb2 preparation by ferricyanide proceeded directly to oxidized flavin, suggesting that the oxidation of reduced FMN by ferricyanide was slower than the subsequent oxidation of the semiquinone (*16*), whereas in Fcb2 the reduced FMN was oxidized by heme $b_2$ faster than the FMN semiquinone (*7*, *13*, *21*).

In order to obtain better insight into the properties of the *S. cerevisiae* FDH domain, we reexamined its mechanism using steady- and pre-steady-state kinetics as well as potentiometric measurements. Our study also disclosed an inhibitory effect of a number of anions, which may influence kinetic results found in the literature.

## MATERIALS AND METHODS

*Enzymes and chemicals. S. cerevisiae* recombinant WT Fcb2 and its recombinant FDH domain were prepared as described earlier in refs *21* and *24*, *27*, respectively, with a few modifications for the domain. DEAE cellulose was replaced by DEAE Sepharose, and a second chromatography on hydroxyapatite was added. Both preparations were stored at −70 °C in 0.1 M phosphate buffer, 1 mM EDTA, pH 7; 10 mM DL-lactate was added to the Fcb2 preparations to keep the enzyme in the reduced state. The holo-enzyme concentrations were expressed as heme concentrations ($\epsilon^{ox}{}_{413}$ = 129 mM$^{-1}$ cm$^{-1}$, $\epsilon^{red}{}_{423}$ = 183 mM$^{-1}$ cm$^{-1}$), and the FDH concentration was determined using $\epsilon_{452}$ = 11 mM$^{-1}$ cm$^{-1}$ for FMN. L-[$^2$H]Lactate (100% deuterium substitution) was synthesized as described previously (*8*). Commercial $Na^+$ pyruvate was recrystallized from water/ethanol. 5-Carba-5-deaza-FMN was a kind gift from Dr. S. Ghisla.

*Kinetic Analysis.* Steady-state kinetics were analyzed at 5 °C, 25 °C, and 30 °C with a Uvikon 943 spectrophotometer, in 0.1 M phosphate buffer, 1 mM EDTA, pH 7.0 ($I$ = 0.22 M), containing specified amounts of added KCl, KBr, $K^+$ acetate, $Na^+$ pyruvate, or excess $Li^+$ L-lactate (50−500 mM). As enzyme concentrations were low (20−40 nM), 10 $\mu$M FMN was added to assay cuvettes in order to stabilize the enzyme. Ferricyanide ($\Delta\epsilon_{420}$ = 1.04 mM$^{-1}$ cm$^{-1}$) was used as acceptor at varying concentrations for experiments at 5 °C in 0.2 cm path length cuvettes. At 25 °C and 30 °C, a single ferricyanide concentration of 13 mM was used for the FDH domain and of 2 mM (saturating) for Fcb2. For determination of $k_{cat}$ and $K_m$ values, experimental points were fitted to a Michaelis−Menten equation with a least-squares iterative nonlinear regression program (Kaleidagraph). Reaction rates were expressed as moles of substrate per mole of FMN per second.

Rapid reaction studies of FDH reduction were performed using a DX.17MV stopped-flow spectrophotometer (Applied Photophysics) at 5 °C. The rate of flavin reduction was monitored at 452 nm. The concentration of FDH after mixing was equal to 10 $\mu$M. Typically, 3−4 kinetic traces were averaged, and analyzed using single-exponential fits. The reoxidation of reduced FMN by ferricyanide (final concentration, 0.7 to 12 mM) at 5 °C was monitored at 480 nm; for these experiments, the FDH domain (final concentration, 10 $\mu$M) in the enzyme syringe was reduced with DL-glyceric acid, a slow substrate for Fcb2 (*28*). In the analysis of reduction or reoxidation rates, the pseudo-first-order rate constants ($k_{app}$) were plotted against L-lactate or ferricyanide concentrations and the data were fitted to a Michaelis−Menten equation or to a linear dependence on concentration. In some reoxidation experiments the FMN absorbance changes were monitored at 520 nm. In the 480−520 nm range, the absorbance changes due to ferricyanide reduction were negligible (less than 1% of those at 420 nm).

*Photoreduction of the FDH Domain.* Domain photoreduction (13−17 $\mu$M) was performed under anaerobic conditions in 0.1 M $K^+$ phosphate buffer, pH 7.0, in the presence or absence of 50 mM pyruvate. 5-Deaza-FMN (0.125 $\mu$M) and EDTA (8 mM) were used as photosensitizers. Before protein introduction from a concentrated stock solution, the solution in a sealed spectrophotometer cuvette was flushed with $O_2$-free argon for 60 min. Subsequently, the cell was irradiated for short periods at 20 °C with a 100 W lamp at a distance of 20 cm; the progress of the reaction was followed spectrophotometrically for 1−2 h. The maximal amount of anionic semiquinone (E-FMN$^{-\bullet}$) formed under irradiation was assumed to be defined by the inflection point of the $A_{380}$ vs $A_{452}$ plot. Under these conditions, the redox

potential of the system at equilibrium at pH 7.0 ($E_7$) is equal to the standard potential of the E-FMN/E-FMNH$^-$ couple ($E°_7$), and [E-FMN] = [E-FMNH$^-$]. The semiquinone concentration may be calculated from eq 1:

$$A_{380} = \epsilon_{380}{}^{sq}[\text{E-FMN}^{-\bullet}] + (\epsilon_{380}{}^{ox} + \epsilon_{380}{}^{red})([E]_{tot} - [\text{E-FMN}^{-\bullet}])/2 \quad (1)$$

where $[E]_{tot}$ is the total enzyme concentration, $\epsilon_{380}{}^{sq}$, $\epsilon_{380}{}^{ox}$, and $\epsilon_{380}{}^{red}$ are the molar extinction coefficients for semiquinone, oxidized and reduced enzyme states. The separation between the two single-electron-transfer potentials was further calculated from the semiquinone formation constant $K$ (eqs 2 and 3):

$$K = [\text{E-FMN}^{-\bullet}]^2/[\text{E-FMN}] \times [\text{E-FMNH}^-], \quad (2)$$

$$E_7(\text{E-FMN/E-FMN}^{-\bullet}) - E_7(\text{E-FMN}^{-\bullet}/\text{E-FMNH}^-) = 59 \text{ mV} \times \log K \quad (3)$$

*Determination of the FDH Domain Standard Redox Potential*. The standard redox potential at pH 7.0 ($E°_7$) was determined at 25 °C using the xanthine/xanthine oxidase reduction system proposed by Massey (*29*), using resorufin ($E°_7 = -0.051$ V) as redox indicator. The cell containing 0.5 mM xanthine, 40 $\mu$M resorufin, and 1 $\mu$M benzylviologen in 0.1 M $K^+$ phosphate, pH 7.0, was made anaerobic as above; 14−16 $\mu$M FDH domain was then introduced in a small volume of concentrated stock solution. The reaction was started by adding 10−20 nM xanthine oxidase. The progress of the reaction was followed in the spectrophotometer. The extent of resorufin reduction was determined by monitoring the absorbance decrease at 570 nm, that of flavin reduction at 452 nm using $\epsilon_{452}{}^{ox} - \epsilon_{452}{}^{red} = 9.9$ mM$^{-1}$ cm$^{-1}$ (*18*), corrected for a decrease in resorufin absorbance ($\Delta A_{452} = 0.059\ \Delta A_{570}$). The FDH domain $E°_7$ was determined from a plot of $\log([FDH_{ox}]/[FDH_{red}])$ vs $\log([\text{resorufin}_{ox}]/[\text{resorufin}_{red}])$. The $E_7$ value was calculated from the Nernst equation (eq 4):

$$E_7 \text{ (V)} = E°_7 + (0.059/n) \log([\text{resorufin}_{ox}]/[\text{resorufin}_{red}]) \quad (4)$$

where $n$ (=2) is the number of electrons transferred.

## RESULTS

*Comparison of Kinetic Parameters between Flavocytochrome $b_2$ and Its Isolated FDH Domain.* In contrast to the numerous kinetic studies of the holo-enzyme (*30*), the studies of the isolated domain are few (*24*, *27*, *31*). We found that the L-lactate:ferricyanide reductase activity of FDH followed a "ping-pong" scheme, resulting in a series of parallel lines of [E]/$v$ vs 1/[lactate] in double reciprocal plots at fixed ferricyanide concentrations as well as vs 1/[ ferricyanide] at fixed lactate concentrations (data not shown). When we determined the kinetic parameters, including the deuterium kinetic isotope effect, under our usual working conditions for the holo-enzyme (0.1 M phosphate buffer, pH 7, 30 °C), we found them to be identical within error to those of the holo-enzyme in terms of $k_{cat}$ and $K_m$ (Table 1). We also determined the steady-state parameters at 5 °C, so as to be able to compare them to those derived from stopped-flow experiments. Table 1 shows $k_{cat}$, $K_m$, and $^DV$ values at 5 °C for the FDH domain that are somewhat higher than for the holo-enzyme.

Table 1: Influence of Reaction Conditions on Steady-State Kinetic Parameters for Lactate Oxidation by the FDH Domain

| enzyme | ref | $k_{cat}$ ($s^{-1}$) | $K_m$ (mM) | $k_{cat}/K_m$ ($s^{-1}$ $mM^{-1}$) | $^DV$ |
|---|---|---|---|---|---|
| 100 mM Phosphate Buffer, 1 mM EDTA, pH 7, 30 °C | | | | | |
| FDH[a] | this work | 259 ± 23 | 0.66 ± 0.13 | 407 ± 122 | 5.4 ± 0.5 |
| holo-enzyme[b] | *21* | 270 | 0.49 | 551 | 4.2 |
| 100 mM Phosphate Buffer, 1 mM EDTA, pH 7, 5 °C | | | | | |
| FDH[a] | this work | 133 ± 1 | 1.18 ± 0.01 | 113 ± 2 | 6.8 ± 0.2 |
| holo-enzyme[b] | this work | 117 ± 1 | 0.89 ± 0.11 | 131 ± 21 | 4.0 |
| 100 mM Phosphate Buffer, 1 mM EDTA, pH 7.5, 25 °C | | | | | |
| FDH[a] | this work | 240 ± 13 | 0.66 ± 0.07 | 363 ± 58 | 6.0 ± 0.1[e] |
| FDH[c] | *31* | 100 | 0.36 | 278 | 3.7 |
| holo-enzyme[b] | *31* | 186 | 0.16 | 1162 | 2.9 |
| 10 mM Tris/HCl Buffer, NaCl to $I$ = 0.1 M, pH 7.5, 25 °C | | | | | |
| FDH[a] | this work | 214 ± 29 | 0.86 ± 0.03 | 249 ± 42 | 7.4 ± 0.8[e] |
| FDH[d] | *24* | 137 | 0.22 | 623 | 3.8 |
| holo-enzyme[b] | *32* | 200 | 0.49 | 408 | 4.7[d] |

[a] 13 mM ferricyanide. [b] 1 or 2 mM ferricyanide. [c] 3 mM ferricyanide. [d] 10 mM ferricyanide. [e] Determined at 20 mM L-lactate, L-($^2$H)lactate, and 13 mM ferricyanide.

Table 2: Stopped-Flow Kinetic Parameters for Flavin Reduction by L-Lactate[a]

| enzyme | $k_{red}$ ($s^{-1}$) | $K_m$ (mM) | $k_{red}/K_m$ ($s^{-1}$ $mM^{-1}$) | $^DV$ |
|---|---|---|---|---|
| FDH | 149 ± 5 | 1.03 ± 0.13 | 145 ± 23 | 7.8 ± 0.2 |
| holo-enzyme[b] | 144 | 0.89 | 162 | 7.2 |

[a] The experiments were carried out in 100 mM phosphate buffer, 1 mM EDTA, pH 7 at 5 °C in the absence of ferricyanide. [b] Taken from ref *21*.

In contrast, two previous studies of the FDH domain had described distinctly lower $k_{cat}$ values for the domain compared to the holo-enzyme, under different experimental conditions (*24*, *31*). When we reproduced these conditions in our laboratory, we found again that the domain was at least as rapid as the holo-enzyme (Table 1).

For the oxidative half-reaction at 5 °C, we found the ferricyanide $K_m{}^{app}$ value to be 1.0 (±0.1) mM, whereas it is lower than 0.1 mM for the holo-enzyme (*16*, *21*). For the heme-free holo-enzyme (*16*) and for a Y143F mutant holo-enzyme in which the mutation significantly slowed down electron transfer between flavin and heme $b_2$ (*21*, *32*), the ferricyanide $K_m{}^{app}$ values were also higher than for the WT holo-enzyme. The difference is due to the fact that, in the latter, heme $b_2$ takes the first electron from FMNH$^-$ more rapidly than does ferricyanide, as rationalized by Iwatsubo et al. (*16*, *17*).

The pre-steady-state kinetics of the FDH domain reduction by L-lactate at 5 °C could be fitted with a single exponential up to 90−95% of the theoretical amplitude. The rates of the second slower phase (1.0−10 $s^{-1}$) did not depend on L-lactate concentration, most probably reflecting a slight inhomogeneity of the FDH preparations. The results are given in Table 2, where it can be seen that they are very similar to those determined independently for the holo-enzyme. The flavin reduction rate $k_{red}$ is also very close to the $k_{cat}$ value obtained at the same temperature (Table 1), confirming that flavin reduction is even more rate-limiting for the isolated domain than for the holo-enzyme.

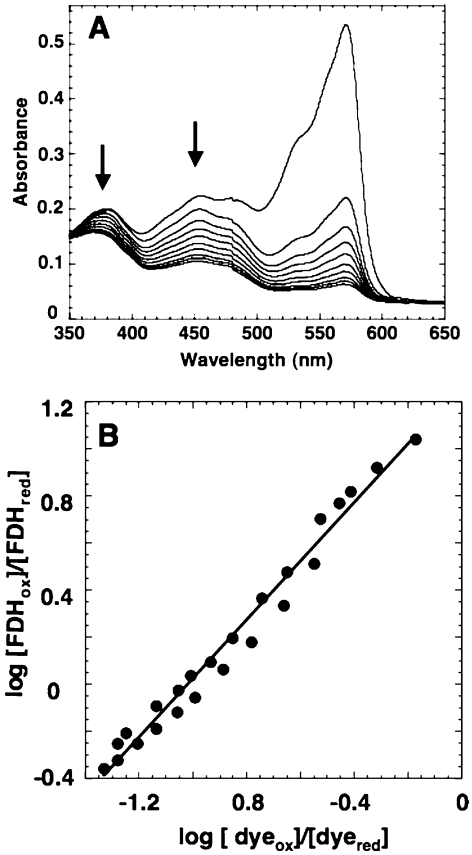


FIGURE 1: Potentiometric titration of the FDH domain. (A) Absorbance changes during potentiometric titration of 18 $\mu$M FDH domain by 40 $\mu$M resorufin, and 1.0 $\mu$M benzyl viologen, in the presence of xanthine and xanthine oxidase, at 25 °C. The spectra were recorded every 20 min. (B) Double-logarithmic plot of the titration data in part A, showing a linear relationship between log [$Fl_{ox}$]/[$Fl_{red}$] and log [resorufin$_{ox}$]/[resorufin$_{red}$].

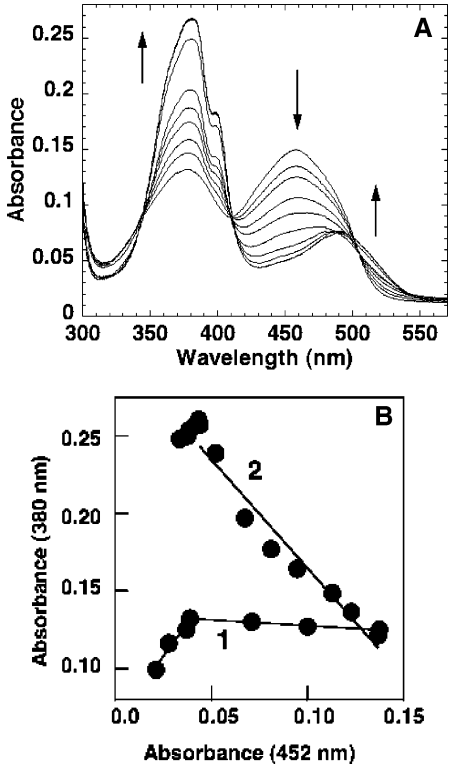


FIGURE 2: Photoreduction of the FDH domain. (A) Photoreduction of 13 $\mu$M FDH by 5-deaza-FMN (0.125 $\mu$M) and EDTA (8 mM) in the presence of 50 mM pyruvate. Each spectrum was recorded after a 0.5−1.0 min irradiation. The final spectrum with highest 380 nm absorbance corresponds to a 10 min irradiation. (B) Relationship between the flavin absorbance changes at 380 and 452 nm during photoreduction in the absence of pyruvate (1) and in the presence of 50 mM pyruvate (2).

Daff et al. (*7*) used the slow substrate glycolate for studying flavocytochrome $b_2$ reoxidation by fast kinetics. Using a similar approach, we used glyceric acid as a slow reductant for the FDH domain (*28*). Typically, after mixing the prereduced FDH domain with ferricyanide, the pseudo-first-order reoxidation rate constants ($k_{app}$) varied between 50 and 300 $s^{-1}$, compared to 0.5 $s^{-1}$ for FDH reduction by 1 mM glyceric acid. Due to the much higher rate of $Fl_{red}$ oxidation by ferricyanide than that of its rereduction by glyceric acid, the amplitude of the absorbance rise at 480 nm was more than 90% of that expected for the complete oxidation of $FMNH^-$ to FMN. At this wavelength, the reaction followed strictly monoexponential kinetics. A biphasic absorbance rise would have indicated the transient formation of E-$FMN^{-\bullet}$. Similarly, we failed to observe a transient increase in absorbance at 520 nm, which may have indicated the formation of anionic semiquinone as the reaction intermediate (see spectrum in Figure 2A). The $k_{app}$ values exhibited a linear dependence on ferricyanide concentration up to the limits imposed by the instrument dead-time (>300 $s^{-1}$), indicating a bimolecular reaction, as for reduced flavin oxidation in heme-free flavocytochrome $b_2$ (*16*). We calculated the bimolecular flavin oxidation rate constant ($k_{ox}$) to be equal to (8.5 ± 0.5) $10^4$ $M^{-1}$ $s^{-1}$.

*Redox Potential of the FMN Prosthetic Group*. According to the most recent potentiometric data for *S. cerevisiae* Fcb2 (*10*), at pH 7.0 and 27 °C, the heme has a standard potential of −3 ± 5 mV, whereas the $E°_7$ of FMN is equal to −90 mV, $E_7$(E-$Fl_{ox}$/E-$Fl_{sq}$) = −45 ± 5 mV, and $E_7$(E-$Fl_{sq}$/E-$Fl_{red}$ = −135 ± 5 mV. This indicates that the FMN semiquinone in the holo-enzyme is stabilized, with an equilibrium constant for semiquinone formation $K$ = 33.5 (eqs 2 and 3). The addition of 10 mM pyruvate resulted in further stabilization of the semiquinone with $K$ = 925 (*10*, *14*). No potentiometric data were available for the isolated FDH domain.

We thus carried out a potentiometric titration of the FDH domain in the presence of resorufin, as described in Materials and Methods. Figure 1A shows a gradual decrease in FMN absorbance at 452 nm, without any transient absorbance increase at 380 nm. The double logarithmic plot (Figure 1B) gives a slope of 1.2, close to the theoretical value of 1.0 for the complete redox equilibrium between the 2-electron-donating dye and the 2-electron-accepting FMN. Under our experimental conditions, 65−70% flavin reduction and 95% resorufin reduction were achieved in *ca.* 3 h. A partial FDH denaturation occurred at longer incubation times. This limited our efforts to slow down the reduction rate by decreasing the xanthine oxidase concentration. Using eq 4, one calculates for the FDH domain, from the data of Figure 1, $E°_7$ = −81 ± 3 mV, in good agreement with the value of −90 mV determined for FMN in the holo-enzyme at 27 °C (*10*).

Photoreduction of the FDH domain in the absence of ligands resulted in an insignificant absorbance increase at 380 nm (Figure 2B curve 1). For the subsequent calculations, $\epsilon_{380}$ values of 9.26 $mM^{-1}$ $cm^{-1}$ (E-$Fl_{ox}$) and 3.55 $mM^{-1}$ $cm^{-1}$ (E-$Fl_{red}$) were determined from the spectra of oxidized and

lactate-reduced FDH domain, respectively; for the semiquinone, we used $\epsilon_{380} = 20.8$ or 18.0 $mM^{-1}$ $cm^{-1}$ as the highest and lowest limit of E-$FMN^{-\bullet}$ absorbance, in view of values reported in the literature (for example, $\epsilon_{384} = 19.4$ $mM^{-1}$ $cm^{-1}$ for L-amino acid oxidase (*33*) and $\epsilon_{374} = 18.0$ $mM^{-1}$ $cm^{-1}$ for glycolate oxidase (*34*)). Using the data of Figure 2B with eqs 1−3, a $K$ value of 1.25−0.64 was calculated. Combined with the results of the potentiometric titration, these figures lead to a difference between the FDH potentials of the first and second electron transfers during FMN reduction of 6 to 11 mV. All these results indicate that the $E_7(Fl_{ox}/Fl_{sq})$ and $E_7(Fl_{sq}/Fl_{red})$ values are very close to each other, in the range of −78 to −86 mV. They also show that the FMN semiquinone state of the FDH domain is significantly destabilized as compared to that of the holoenzyme (*10*).

FDH domain photoreduction experiments were also performed in the presence of 50 mM pyruvate. In this case, the absorbance decrease at 450 nm was accompanied by a marked absorbance increase at 380 nm with isosbestic points at 410 and 502 nm (Figure 2A and 2B curve 2), features which are typical of the formation of a red (anionic) FMN semiquinone (*33*, *34*). The highest absorbance at 380 nm was reached after a 10 min irradiation (Figure 2A); there was then a slow decay by about 5% in a subsequent 1 to 1.5 h irradiation. Assuming a stoichiometric formation of semiquinone, we calculated an $\epsilon_{380}$ value of 20.8 $mM^{-1}$ $cm^{-1}$, in good agreement with the literature values reported above. These photoreduction experiments indicate that pyruvate stabilizes the flavin semiquinone state of FDH as it does in the holo-enzyme (*9*). The anionic semiquinone states of homologous lactate oxidase (*35*) and lactate monooxygenase (*36*) were also reported to be stabilized by pyruvate.

*FDH Domain Inhibition Studies*. As mentioned in the introduction, Fcb2 is known to be inhibited by the reaction product, pyruvate, and by high substrate concentrations. These inhibitions were ascribed to substrate and product binding not only to the oxidized enzyme but also to the enzyme when the flavin is in the semiquinone state (*14*, *21*). More recently, an inhibition at high acetate concentration was ascribed to an ionic strength effect (*21*). As the effect was more marked with a Y143F mutant enzyme, for which electron transfer to the heme is considerably slowed down (*21*, *32*), it could not be decided if the stronger inhibition was due to the mutation or to the mutation-induced uncoupling between the domains. It thus appeared of interest to study these inhibitions with the isolated flavin domain.

In the steady state, in the presence of pyruvate, the reduction of ferricyanide by the FDH domain also followed a ping-pong pattern (data not shown). At varied L-lactate concentrations and a fixed ferricyanide concentration, pyruvate behaved as a mixed-type inhibitor toward L-lactate (Figure 3). Secondary plots yielded $K_i = 6$ mM and $K_i' = 40$ mM. A similar mixed inhibition pattern was also observed toward ferricyanide at a fixed L-lactate concentration with $K_i = 11$ mM and $K_i' = 27$ mM (Figure 3).

Next, the effects of pyruvate were examined in pre-steady-state kinetic studies of the FDH domain reduction and reoxidation. Pyruvate acted as a competitive inhibitor of L-lactate for FDH reduction (Figure 4), with $K_i = 9.7 \pm 1.2$ mM. In stopped-flow reoxidation experiments with ferricyanide, the flavin $k_{ox}$ was decreased to $(4.0 \pm 0.5) \times 10^4$ $M^{-1}$ $s^{-1}$ and to $(2.2 \pm 0.2) \times 10^4$ $M^{-1}$ $s^{-1}$ in the presence of 50 mM and 100 mM pyruvate, respectively (Table 4). Pyruvate did not alter the monoexponential character of FMN reoxidation, monitored at 480 nm, and did not change noticeably the amplitude of the absorbance rise, as compared with the reoxidation data in the absence of pyruvate. However, in the presence of 50−100 mM pyruvate, we detected an absorbance rise at 520 nm, which appeared during the instrument dead time and amounted to 4−7% of the absorbance increase at 480 nm. The rate of its subsequent decay was similar to that determined at 480 nm.

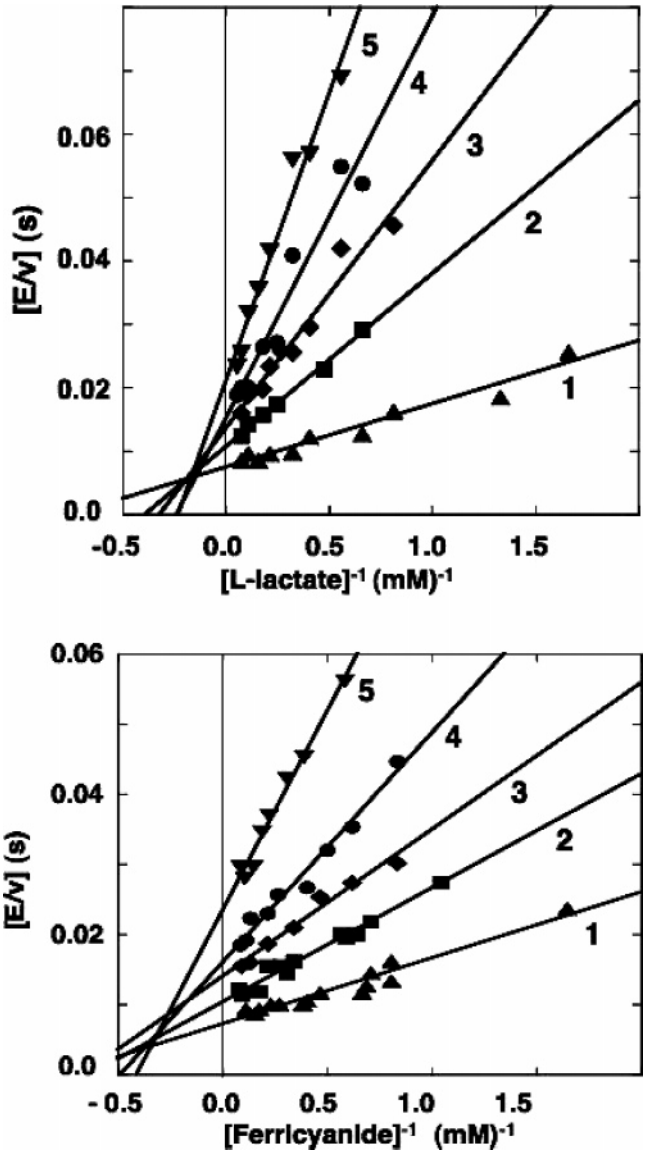


FIGURE 3: Inhibition of the FDH domain by pyruvate in the steady state. Top: 10 mM ferricyanide and variable L-lactate; pyruvate concentrations: 0 mM (1), 10 mM (2), 20 mM (3), 30 mM (4), and 50 mM (5), in 0.1 M phosphate buffer, pH 7.0 at 5 °C. Bottom: 10 mM L-lactate and variable ferricyanide concentrations; pyruvate concentrations: 0 mM (1), 10 mM (2), 20 mM (3), 30 mM (4), and 50 mM (5), in 0.1 M phosphate buffer, pH 7.0 at 5 °C.

High concentrations of chloride, bromide, acetate, and phosphate, as well as marked excess L-lactate, inhibited the FDH domain turnover. The inhibition mode of the salts was similar to that of pyruvate insofar as both $k_{cat}$ and $k_{cat}/K_m$ values for lactate were affected. Table 3 gives values of these

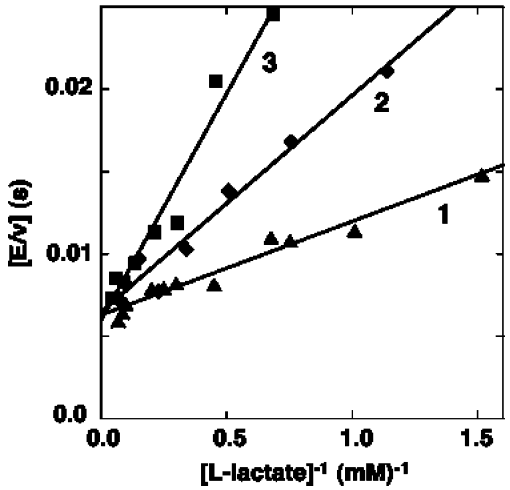


FIGURE 4: Kinetics of the pre-steady-state reduction of the FDH domain by L-lactate in the absence (1) and in the presence of 25 mM (2) and 50 mM (3) pyruvate.

Table 3: Influence of Anions on the FDH Domain Steady-State Kinetic Parameters[a]

| additions | $k_{cat}$ ($s^{-1}$) | $K_m$ (mM) | $k_{cat}/K_m$ ($s^{-1}$ $mM^{-1}$) |
|---|---|---|---|
| none[b] | 133 ± 1 | 1.2 ± 0.1 | 113 ± 2 |
| 300 mM phosphate[c] | 101 ± 1 | 2.8 ± 0.1 | 36 ± 1 |
| 400 mM $K^+$ acetate | 86 ± 1 | 4.6 ± 0.1 | 19 ± 1 |
| 400 mM $K^+$ chloride | 60 ± 1 | 2.3 ± 0.1 | 26 ± 1 |
| 400 mM $K^+$ bromide | 45 ± 1 | 4.0 ± 0.1 | 11 ± 1 |

[a] The experiments were carried out in 100 mM phosphate buffer, 1 mM EDTA, pH 7 at 5 °C, at variable L-lactate concentrations and constant 10 mM ferricyanide. [b] Taken from Table 1. [c] Final phosphate concentration.

Table 4: Influence of Anions on Ferricyanide Reduction by the Reduced FDH Domain[a]

| addition | $k_{red}$ ($M^{-1}$ $s^{-1}$) |
|---|---|
| none | $(8.5 \pm 0.5) \times 10^4$ |
| 50 mM $Na^+$ pyruvate | $(4.0 \pm 0.5) \times 10^4$ |
| 100 mM $Na^+$ pyruvate | $(2.2 \pm 0.2) \times 10^4$ |
| 400 mM $K^+$ acetate | $(5.2 \pm 0.4) \times 10^4$ |
| 400 mM $K^+$ chloride | $(3.6 \pm 0.3) \times 10^4$ |

[a] The experiments were carried out in 100 mM phosphate buffer, 1 mM EDTA, pH 7 at 5 °C in the stopped-flow instrument. The enzyme was prereduced with 1 mM DL-glyceric acid, as described in Materials and Methods.

parameters obtained at a fixed high salt concentration and a single ferricyanide concentration. The salts as well as high L-lactate concentrations decreased the $k_{cat}/K_m$ value for ferricyanide as variable substrate. The dependence of $k_{cat}/K_m$ on salt or L-lactate concentration gave almost linear Cleland plots (Figure 5), indicating that efficiency of inhibition decreased in the order pyruvate $\gg$ $Br^-$ > L-lactate > $Cl^-$ > phosphate $\sim$ acetate.

On the other hand, in pre-steady-state experiments, chloride and acetate behaved as competitive inhibitors of L-lactate (data not shown), with $K_i$ values of 450 ± 60 mM and 170 ± 80 mM, respectively. High L-lactate concentrations (100−300 mM) did not decrease the flavin reduction rate, as already observed for the holo-enzyme (*21*). In pre-steady-state reoxidation experiments of the domain, acetate and chloride decreased the ferricyanide reduction rate, as shown in Table 4.

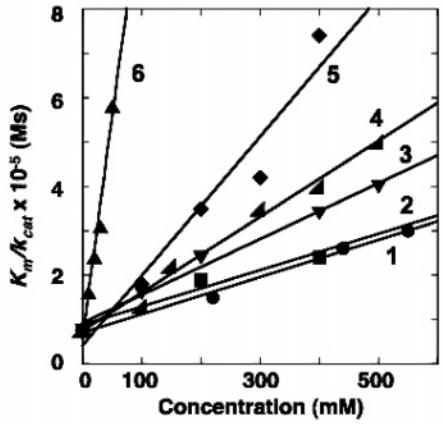


FIGURE 5: Effect of anions on $k_{cat}/K_m$ for ferricyanide with the increase in salt concentration. The reaction was carried out in 0.1 M $K^+$ phosphate buffer, pH 7.0, 10 mM L-lactate. Additions: phosphate (1), acetate (2), chloride (3), L-lactate (4), bromide (5), pyruvate (6).

*Effects of Anions on the Kinetics of Holo-Flavocytochrome $b_2$ and Its R289K Mutant Form.* Since the anions used in this work appeared to inhibit the FDH domain with a kinetic pattern similar to that of pyruvate, it appeared that they may have a common binding site close to the flavin. The first Fcb2 crystal structure showed pyruvate bound at the active site with its carboxylate group engaged in an electrostatic interaction with R376 and in a hydrogen bond with Y143 (Figure 6) (*4*). In addition, in the structure of the recombinant WT enzyme−sulfite complex (*37*) as well as in that of the Y143F mutant enzyme complex with pyruvate (*38*), it appeared that R289 could reorient itself (from the so-called distal orientation to the so-called proximal orientation), so as to interact with the negatively charged ligand. Moreover, in the crystal structure of the FDH domain, R289 also adopts the proximal orientation in part of the subunits (Figure 6) (*25*). Finally, study of the R289K mutant enzyme indicated that R289 participates in transition state stabilization and must contribute to the binding of a number of active-site ligands (*39*). It was also shown that pyruvate is a purely competitive inhibitor for the mutant enzyme, which is not sensitive anymore to inhibition by excess lactate. It thus appeared of interest to check whether the effect of the mutation extended to the binding of other anions. The case was investigated by comparing the WT and R289K holo-enzymes.

The results are presented in Table 5. It is clear that for the WT holo-enzyme, high concentrations of acetate, phosphate, chloride, and bromide inhibit ferricyanide reduction by influencing both $k_{cat}$ and $k_{cat}/K_m$ values in the usual ferricyanide reduction test. In contrast, for the mutant enzyme, they appear to have no influence, within error. It was confirmed that pyruvate is a strictly competitive inhibitor ($K_i$ = (26 ± 9) mM at 5 °C, comparable to the value of 39 mM determined at 30 °C (*39*)). It thus appears that the mutant enzyme capacity to bind anions has been severely impaired if not lost.

## DISCUSSION

The data of the present work enabled us to clarify some important features of the reactions catalyzed by the Fcb2 FDH domain.

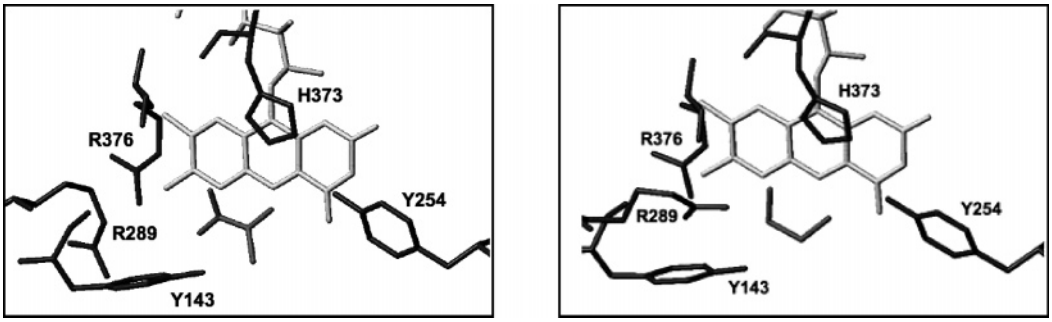


FIGURE 6: Flavocytochrome $b_2$ active-site residues. Left: Pyruvate bound in the holo-enzyme subunit B (1KBI). The flavin is in the semiquinone form (*4*); R289 is in the distal orientation Right: Ethylene glycol from the mother liquors bound in subunit B of the FDH domain structure (1KBJ). The flavin is in the oxidized form; R289 adopts the proximal orientation; in subunit A, the two orientations are present. This figure was prepared using Turbo-Frodo (*50*).

Table 5: Influence of Anions on the Steady-State Kinetic Parameters of WT and R289K Mutant Flavocytochrome $b_2$[a]

| addition | WT flavocytochrome $b_2$ | | | R289K mutant flavocytochrome $b_2$ | | |
|---|---|---|---|---|---|---|
| | $k_{cat}$ ($s^{-1}$) | $K_m$ (mM) | $k_{cat}/K_m$ ($s^{-1}$ $mM^{-1}$) | $k_{cat}$ ($s^{-1}$) | $K_m$ (mM) | $k_{cat}/K_m$ ($s^{-1}$ $mM^{-1}$) |
| none[b] | $117 \pm 0.4$ | $0.89 \pm 0.11$ | $131 \pm 21$ | $8.6 \pm 0.5$ | $7.0 \pm 0.5$ | $1.23 \pm 0.16$ |
| 200 mM phosphate[c] | $71 \pm 2$ | $0.90 \pm 0.12$ | $79 \pm 13$ | $9.2 \pm 0.4$ | $8.7 \pm 1.2$ | $1.06 \pm 0.19$ |
| 400 mM $K^+$ acetate | $113 \pm 3$ | $2.7 \pm 0.2$ | $42 \pm 4$ | $8.8 \pm 0.5$ | $9.2 \pm 1.3$ | $0.96 \pm 0.19$ |
| 400 mM $K^+$ chloride | $75 \pm 4$ | $1.5 \pm 0.3$ | $50 \pm 14$ | $9.2 \pm 0.2$ | $6.5 \pm 0.4$ | $1.41 \pm 0.12$ |
| 400 mM M $K^+$ bromide | $61 \pm 3$ | $0.94 \pm 0.19$ | $65 \pm 16$ | $7.8 \pm 0.2$ | $5.8 \pm 0.5$ | $1.34 \pm 0.2$ |

[a] The experiments were carried out in 0.1 M phosphate buffer, 1 mM EDTA, pH 7 at 5 °C, at varying L-lactate concentrations in the presence of 1.5 and 2 mM ferricyanide for the WT and the mutant enzymes, respectively. [b] This work (taken from Table 1 for the WT enzyme). [c] Final phosphate concentration.

*Kinetic and Potentiometric Characterization of the FDH Domain*. In steady-state experiments, the $k_{cat}$ values with respect to lactate are, under a variety of buffer and temperature conditions, practically identical with those we determined for the holo-enzyme (Table 1). In contrast, other investigators found distinctly lower $k_{cat}$ values for the domain than for the holo-enzyme, values which are also lower than the ones we obtained when we used their conditions (*24*, *31*) (Table 1). A possible explanation for these differences is the relative instability of the domain. We found that it rapidly lost activity at concentrations of $\sim$10−20 $\mu$M, so that we routinely added 10 $\mu$M FMN to these dilutions as well as to the assay cuvettes, where the enzyme is 20−40 nM. The $K_m^{app}$ value for ferricyanide is high relative to that of the holo-enzyme, as was found with the heme-free flavocytochrome $b_2$ (*16*) and the recombinant domain under different buffer conditions (*24*).

There is *a priori* no compelling reason for having similar steady-state rates ($k_{cat}$) of lactate oxidation for the two flavodehydrogenase forms, since, as mentioned before, the acceptors for the two monoelectronic oxidative half-reactions are different, and therefore the actual transfer rates may be different. The rationale for the rate similarity is given by the values of the kinetic deuterium isotope effects. They show flavin reduction to be the main rate-limiting step in the holo-enzyme turnover, at least under our experimental conditions (*8*, *15*) (see below for further discussion). The fact that we measured a pre-steady-state rate for the FDH domain which is close to that determined in the steady state suggests that flavin reduction may be even be more rate-limiting for the domain than for the holo-enzyme. The values of the present kinetic isotope effects as well as the high rate constant for ferricyanide reduction by $FMNH^-$ support this idea.

The data on the FDH domain photoreduction and redox potentiometry (Figures 1 and 2) indicate that the flavin $E°_7$ is practically the same as that in the holo-enzyme (*10*), whereas its semiquinone state is markedly destabilized. This difference is unexpected in view of the mobility of the heme domain relative to the tetrameric FDH domain core (*4*, *40*). Accumulated observations suggesting the independence of the domains is summarized in ref *30*. At the present resolution of 2.3 to 2.5 Å, the crystal structures of the independent domain and of the holo-enzyme domain do not differ significantly (*4*, *25*) but one cannot exclude that atomic resolution would not disclose differences. Another possibility is that it is the presence of the heme domain, however mobile, with its capacity to act as an electron sink, that stabilizes the $Fl_{sq}$ form. The amplitude and frequency of the heme domain movements are unknown at present. Altogether, the origin of the difference in semiquinone stability between the FDH domain and the holo-enzyme is unclear. There exists at least one precedent of an inverse situation. Gao et al. (*41*) found that, in spite of a similar redox potential for the isolated nNOS flavin domain and the holo-enzyme, the separation between the FMN half-reduction potentials is larger in the former than in the latter.

During the reoxidation of the reduced FDH domain by ferricyanide, there is no observable transient formation of FMN semiquinone, which again agrees with the data on the oxidation of heme-free flavocytochrome $b_2$ (*16*). This shows that the oxidation of E-$Fl_{sq}$ by ferricyanide is faster than the oxidation of E-$Fl_{red}$, the latter being the rate-limiting step in the reoxidation. The rate constant of reduced flavin domain oxidation by ferricyanide, $(0.85 \pm 0.05) \times 10^5$ $M^{-1}$ $s^{-1}$ at 5 °C, is not too different from the $k_{cat}/K_m$ value of $(1.1 \pm 0.2) \times 10^5$ $M^{-1}$ $s^{-1}$ we determined at variable ferricyanide concentrations in steady-state experiments, at the same temperature.

In holo-flavocytochrome $b_2$, the faster $FMNH^-$ to heme than $FMN^{-\bullet}$ to heme electron transfer may be explained by the fact that the potential of the E-FMN/E-$FMN^{-\bullet}$ couple is 90 mV higher than that of E-$FMN^{-\bullet}$/E-$FMNH^-$ (*10*). The significant semiquinone destabilization in the FDH domain (Figures 1 and 2), with a difference of only 6 to 11 mV between the two states, may explain the faster oxidation of $FMN^{-\bullet}$ than of $FMNH^-$. Since, however, the acceptors for the flavin-derived reducing equivalents are in one case a small charged inorganic molecule, in the other case a protein-bound heme, other factors, electrostatic or steric ones, may come into play.

*Inhibition of the FDH Domain by Pyruvate.* Fcb2 inhibition by the product has been the object of numerous studies in the past, with some conflicting results. A steady-state study with ferricyanide as acceptor indicated a complex situation: competitive inhibition at low concentrations ($K_i$ = 3 mM) and noncompetitive inhibition at higher concentrations ($K_i$ = 30 mM) (*18*). With the *H. anomala* Fcb2, the inhibition was noncompetitive at the lowest concentrations, uncompetitive at the highest ones (*14*); this was ascribed to tighter pyruvate binding to the $Fl_{sq}$ state than to $Fl_{ox}$ and $Fl_{red}$ states. With Fcb2 from both yeast strains, it was shown that pyruvate binding stabilizes the $Fl_{sq}$ state, and alters the potential of the $Fl_{sq}/Fl_{red}$ and $Fl_{ox}/Fl_{sq}$ couples (*9*, *14*, *42*). The inhibition of heme reduction by pyruvate was ascribed to the significant increase of the $Fl_{ox}/Fl_{sq}$ redox potential, leading to a decreased driving force for transfer between $Fl_{sq}$ and heme $b_2$ (*10*, *14*). It was proposed that the pyruvate−$Fl_{sq}$ complex was a dead-end complex incapable of transferring electrons to monoelectronic acceptors such as heme $b_2$ and ferricyanide. Indeed, with *S. cerevisiae* Fcb2, Daff et al. (*7*) found that pyruvate inhibited pre-steady-state flavin reoxidation with a $K_i$ value of 40 mM. In contrast, Walker and Tollin interpreted flash photolysis results as indicating that pyruvate was favoring electron transfer from reduced heme to $Fl_{ox}$ (*43*, *44*), but inhibited electron transfer from $Fl_{red}$ to heme (*42*).

Our findings enable us to clarify certain important aspects of the inhibition of Fcb2 by pyruvate, by simplifying the system. Indeed, the most commonly used assay in the steady-state studies of Fcb2 is an enzyme-catalyzed reduction of ferricyanide by L-lactate. However, the $k_{cat}$ of this reaction is under the control of the major rate-limiting step of FMN reduction by L-lactate (*8*, *15*) and, depending on reaction conditions, of electron transfer from FMN semiquinone to heme (*7*). Besides, the low ferricyanide $K_m$ (<0.1 mM (*16*, *21*) complicates the inhibition studies of the enzyme oxidative half-reaction.

With the FDH domain, while in the steady state pyruvate was a mixed type inhibitor with respect both to lactate and to ferricyanide **(**Figure 3**)**, in the pre steady state it behaved as a competitive inhibitor of FMN reduction by L-lactate (Figure 4) and it inhibited $FMNH^-$ reoxidation by ferricyanide (Table 4). These inhibition features reflect pyruvate binding to the oxidized and reduced flavin, respectively. The inhibition patterns of steady-state kinetics of FDH (Figure 3) may be understood using a "ping-pong" scheme of FDH catalysis, accompanied by product inhibition (eq 5), where S is L-lactate, P the reaction product, pyruvate, and Q is ferricyanide. This scheme implies the binding of pyruvate to all three oxidation states of E-FMN.

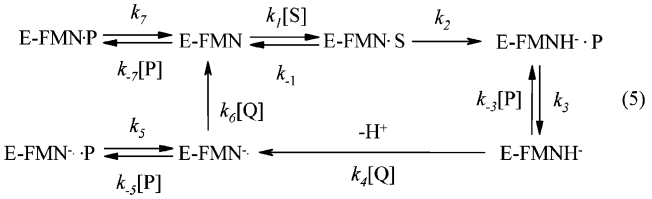


(5)

The resulting steady-state rate expression (eq 6) shows that pyruvate must decrease $k_{cat}/K_m$ of L-lactate ($k_1k_2/k_{-1} + k_2$ in eq 5), and the rate constants of E-$FMNH^-$ and E-$FMN^{-\bullet}$ oxidation by ferricyanide, $k_4$ and $k_6$:

$$\frac{[E]}{v} = \frac{1}{k_2}\left(1 + \frac{k_{-1} + k_2}{k_1[S]}\left(1 + \frac{k_{-7}[P]}{k_7}\right)\right) + \frac{1}{k_6[Q]}\left(1 + \frac{k_{-5}[P]}{k_5}\right) + \frac{1}{k_3} + \frac{1}{k_4[Q]}\left(1 + \frac{k_{-3}[P]}{k_3}\right) \quad (6)$$

As observed above, the steady-state $k_{cat}/K_m$ for ferricyanide is close to $k_4$, the rate constant of E-$FMNH^-$ oxidation, which implies that $k_6 \gg k_4$. Equation 6 may then be simplified (eq 7):

$$\frac{[E]}{v} = \frac{1}{k_2}\left(1 + \frac{k_{-1} + k_2}{k_1[S]}\left(1 + \frac{k_{-7}[P]}{k_7}\right)\right) + \frac{1}{k_3} + \frac{1}{k_4[Q]}\left(1 + \frac{k_{-3}[P]}{k_3}\right) \quad (7)$$

which shows that the presence of pyruvate should also decrease the $k_{cat}/K_m$ of ferricyanide (Figure 3). The pyruvate $K_i$ values determined from the slopes of double-reciprocal plots, 6 mM (vs L-lactate) and 11 mM (vs ferricyanide), correspond to pyruvate binding to oxidized and two-electron-reduced forms of FDH. In view of the significant E-$Fl_{sq}$ stabilization by pyruvate (Figure 2), one might expect some amount of FMN semiquinone to be observed during the reoxidation in the presence of pyruvate. Nevertheless, the presence of pyruvate did not alter the monophasic character of reoxidation of E-$FMNH^-$ by ferricyanide, monitored at 480 nm, and did not noticeably affect the amplitude of the absorbance rise. The negligible increase in 520 nm absorbance, which appeared during the dead-time of the instrument, is most probably due to complex formation of pyruvate with E-$Fl_{red}$.

*Inhibition of the FDH Domain by Anions.* In a previous study (*21*), it was suggested that the Fcb2 inhibition by excess L-lactate was due to lactate binding weakly to the semiquinone state, while the effect of high acetate concentrations was analyzed as an ionic strength effect. The present results point to a somewhat different conclusion.

The data of Figure 5 indicate that the various salts studied in this work exhibit a different inhibition efficiency independently of ionic strength. This points to a specific binding of anions at the enzyme active site. Moreover, the kinetic effects of excess L-lactate and anions closely resemble the FDH inhibition patterns given by pyruvate (Figure 5). In pre-steady-state kinetic experiments, anions at high concentrations behaved as competitive inhibitors toward L-lactate and ferricyanide. Thus, the inhibition exerted by high L-lactate concentrations and anions is formally analogous to the inhibition by pyruvate (eqs 5−7), with formation of dead-

end complexes with E-FMN (anions), and E-FMNH$^-$ (anions, excess L-lactate). The present results may explain a discrepancy between kinetic data obtained in phosphate buffer and other ones in Tris/HCl with ionic strength adjusted with NaCl. Indeed, according to Daff et al. (*13*), in the Fcb2 turnover with cytochrome *c* under the latter conditions, the slowest step is electron transfer from Flsq to heme $b_2$, and not any more flavin reduction by lactate, as in phosphate buffer (*7*). Since, according to the present results, chloride is a more efficient inhibitor than phosphate (Figure 5), one may wonder whether the discrepancy does not arise from the difference in the ionic composition of the buffers.

*A Binding Site for Anions*. Fcb2 crystal structures indicated that the pyruvate carboxylate forms a hydrogen bond with Y143 and R376, as well as an electrostatic interaction with the latter. In addition, as detailed above, the R289 side chain is mobile and can interact with ligands in the active site, especially negatively charged ones (Figure 6). Previous work on R289K Fcb2 (*39*) disclosed that the mutant enzyme had lost the inhibition by excess substrate and that the inhibition by pyruvate has become purely competitive in the steady state. The present work indicates that binding of the other anions to oxidized and reduced enzymes has also been lost. Altogether, we can thus conclude that indeed anions occupy part of the lactate−pyruvate binding site and that R289, as well as R376 and Y143, contributes to the binding. The three side chains are invariant in the Fcb2 family enzymes, with the exception of Y143 which is sometimes a phenylalanine as in long-chain hydroxy acid oxidase (*45*); thus, one may expect the family members to possess a similar site. Indeed, the solution studies of Schuman and Massey (*46*, *47*) suggested the existence of a specific binding of anions to pig liver glycolate oxidase. Moreover, the crystal structures of long-chain hydroxy acid oxidase and of mandelate dehydrogenase presented acetate (*48*) and a sulfate ion (*49*), respectively, bound at the active site, anions that were present in the mother liquors at high concentrations. In the structure of long-chain hydroxy acid oxidase, the acetate carboxylate interacts with the homologues of R289 and Y254 (*48*). In the high-resolution structure of both oxidized and reduced mandelate dehydrogenase, the sulfate ion forms interactions with the two active-site arginines, the catalytic histidine and water molecules (*49*). Thus, depending on the enzyme and on the structure of the ligand, there are variable possibilities for ionic interactions and hydrogen bonding in the active sites of this enzyme family.

## ACKNOWLEDGMENT

The authors are indebted to Dr. C. Capeillère-Blandin for a critical reading of the manuscript.

## REFERENCES

1. Daum, G., Böhni, P. C., and Schatz, G. (1982) Import of proteins into mitochondria. Cytochrome $b_2$ and cytochrome *c* peroxidase are located in the intermembrane space of yeast mitochondria, *J. Biol. Chem. 257*, 13028−13033.
2. Appleby, C. A., and Morton, R. K. (1954) Crystalline cytochrome *b*, and lactic dehydrogenase of yeast, *Nature 173*, 749−752.
3. Jacq, C., and Lederer, F. (1974) Cytochrome $b_2$ from baker's yeast (L-lactate dehydrogenase). A double-headed enzyme, *Eur. J. Biochem. 41*, 311−320.
4. Xia, Z. X., and Mathews, F. S. (1990) Molecular structure of flavocytochrome $b_2$ at 2.4 Å resolution, *J. Mol. Biol. 212*, 837−863.
5. Capeillère-Blandin, C., Bray, R. C., Iwatsubo, M., and Labeyrie, F. (1975) Flavocytochrome $b_2$ : kinetic studies by absorbance and electron paramagnetic resonance spectroscopy of electron distribution among prosthetic groups, *Eur. J. Biochem. 54*, 549−566.
6. Čénas, N., Pocius, A. K., Butkus, A. A., Kulys, J. J., and Antanavicius, V. S. (1986) Kinetics of cytochrome $b_2$ oxidation by electron acceptors, *Biokhimyia 51*, 285−292.
7. Daff, S., Ingledew, W. J., Reid, G. A., and Chapman, S. K. (1996) New insights into the catalytic cycle of flavocytochrome $b_2$, *Biochemistry 35*, 6345−6350.
8. Pompon, D., Iwatsubo, M., and Lederer, F. (1980) Flavocytochrome $b_2$ (baker's yeast). Deuterium isotope effect studied by rapid-kinetic methods as a probe for the mechanism of electron transfer, *Eur. J. Biochem. 104*, 479−488.
9. Tegoni, M., Janot, J. M., and Labeyrie, F. (1986) Regulation of dehydrogenase/one-electron transferases by modification of flavin redox potentials. Effects of product binding on semiquinone stabilization in yeast flavocytochrome $b_2$, *Eur. J. Biochem. 155*, 491−503.
10. Tegoni, M., Silvestrini, M. C., Guigliarelli, B., Asso, M., Brunori, M., and Bertrand, P. (1998) Temperature-jump and potentiometric studies on recombinant wild type and Y143F and Y254F mutants of *Saccharomyces cerevisiae* flavocytochrome $b_2$ : role of the driving force in intramolecular electron-transfer kinetics, *Biochemistry 37*, 12761−12771.
11. Capeillère-Blandin, C. (1982) Transient kinetics of the one-electron-transfer reaction between reduced flavocytochrome $b_2$ and oxidized cytochrome *c*. Evidence for the existence of a protein complex in the reaction, *Eur. J. Biochem. 128*, 533−542.
12. Capeillère-Blandin, C. (1995) Flavocytochrome $b_2$-cytochrome *c* interactions: The electron-transfer reaction revisited, *Biochimie 77*, 516−530.
13. Daff, S., Sharp, R. E., Short, D. M., Bell, C., White, P., Manson, F. D. C., Reid, G. A., and Chapman, S. K. (1996) Interaction of cytochrome *c* with flavocytochrome $b_2$, *Biochemistry 35*, 6351−6357.
14. Tegoni, M., Janot, J. M., and Labeyrie, F. (1990) Inhibition of L-lactate cytochrome *c* reductase (flavocytochrome $b_2$) by product binding to the semiquinone transient: loss of reactivity toward monoelectronic acceptors, *Eur. J. Biochem. 190*, 329−342.
15. Pompon, D. (1980) Flavocytochrome $b_2$ from baker's yeast. Computer-simulation studies of a new kinetic scheme for intramolecular electron transfer, *Eur. J. Biochem. 106*, 151−159.
16. Iwatsubo, M., Mevel-Ninio, M., and Labeyrie, F. (1977) Rapid kinetic studies of partial reactions in the heme-free derivative of L-lactate cytochrome *c* oxidoreductase (flavocytochrome $b_2$); the flavodehydrogenase function, *Biochemistry 16*, 3558−3566.
17. Iwatsubo, M., and Capeillère, C. (1967) Cytochrome $b_2$ (L-lactate déshydrogénase): équilibre et processus élémentaires de la réaction de combinaison du substrat à l'enzyme, *Biochim. Biophys. Acta 146*, 349−366.
18. Lederer, F. (1978) Sulfite binding to a flavodehydrogenase, cytochrome $b_2$ from baker's yeast, *Eur. J. Biochem. 88*, 425−431.
19. Somlo, M., and Slonimski, P. P. (1966) Différence entre les propriétés de la L-lactico-déshydrogénase physiologique et la L-lactico-déshydrogénase cristallisée de la levure. *Bull. Soc. Chim. Biol. 48*, 1221−1249.
20. Thusius, D., Blazy, B., and Baudras, A. (1976) Mechanism of yeast cytochrome $b_2$ action. I. Thermodynamics and relaxation kinetics of the interaction between cytochrome $b_2$ and oxalate, *Biochemistry 15*, 250−256.
21. Rouvière, N., Mayer, M., Tegoni, M., Capeillère-Blandin, C., and Lederer, F. (1997) Molecular interpretation of inhibition by excess substrate in flavocytochrome $b_2$: a study with wild-type and Y143F mutant enzymes, *Biochemistry 36*, 7126−7135.
22. Tegoni, M., Gervais, M., and Desbois, A. (1997) Resonance Raman study on the oxidized and anionic semiquinone forms of flavocytochrome $b_2$ and L-lactate monooxygenase. Influence of the structure and environment of the isoalloxazine ring on the flavin function, *Biochemistry 36*, 8932−8946.
23. Celerier, J., Risler, Y., Schwencke, J., Janot, J. M., and Gervais, M. (1989) Isolation of the flavodehydrogenase domain of *Hansenula anomala* flavocytochrome $b_2$ after mild proteolysis by an *H. anomala* proteinase, *Eur. J. Biochem. 182*, 67−75.

24. Balme, A., Brunt, C. E., Pallister, R., Chapman, S. K., and Reid, G. A. (1995) Isolation and characterization of the flavin-binding domain of flavocytochrome $b_2$, expressed independently in *Escherichia coli*, *Biochem. J. 309*, 601−605.
25. Cunane, L. M., Barton, J. D., Chen, Z. W., Welsh, F. E., Chapman, S. K., Reid, G. A., and Mathews, F. S. (2002) Crystallographic study of the recombinant flavin-binding domain of baker's yeast flavocytochrome $b_2$: Comparison with the intact wild-type enzyme, *Biochemistry 41*, 4264−4272.
26. Forestier, J. P., and Baudras, A. (1971) On the role of the prosthetic heme groups of cytochrome $b_2$ in the transfer of electrons from L-lactate to ferricyanide and cytochrome *c*, in *Flavins and Flavoproteins* (Kamin, H., Ed.) pp 599−605, University Park Press, Baltimore.
27. Balme, A., and Lederer, F. (1994) On the rate of proton exchange with solvent of the catalytic histidine in flavocytochrome $b_2$ (yeast L-lactate dehydrogenase), *Protein Sci. 3*, 109−117.
28. Urban, P., Alliel, P. M., and Lederer, F. (1983) On the transhydrogenase activity of baker's yeast flavocytochrome $b_2$, *Eur. J. Biochem. 134*, 275−281.
29. Massey, V. (1991) A simple method for the determination of redox potentials, in *Flavins and Flavoproteins 1990* (Curti, B., Ronchi, S., and Zanetti, G., Eds.) pp 59−66, Walter de Gruyter, Berlin, New York.
30. Lederer, F. (1991) Flavocytochrome $b_2$, in *Chemistry and Biochemistry of Flavoenzymes* (Müller, F., Ed.) pp 153−242, CRC Press, Boca Raton, FL.
31. Sobrado, P., Daubner, S. C., and Fitzpatrick, P. F. (2001) Probing the relative timing of hydrogen abstraction steps in the flavocytochrome $b_2$ reaction with primary and solvent deuterium isotope effects and mutant enzymes, *Biochemistry 40*, 994−1001.
32. Miles, C. S., Rouvière-Fourmy, N., Lederer, F., Mathews, F. S., Reid, G. A., Black, M. T., and Chapman, S. K. (1992) Tyrosine 143 facilitates interdomain electron transfer in flavocytochrome $b_2$, *Biochem. J. 285*, 187−192.
33. Stankovich, M. T., and Fox, B. G. (1984) Redox potential-pH properties of the flavoprotein L-amino-acid oxidase, *Biochim. Biophys. Acta 786*, 49−56.
34. Pace, C., and Stankovich, M. (1986) Oxidation−reduction properties of glycolate oxidase, *Biochemistry 25*, 2516−2522.
35. Maeda-Yorita, K., Aki, K., Sagai, H., Misaki, H., and Massey, V. (1995) L-lactate oxidase and L-lactate monooxygenase: mechanistic variations on a common structural theme, *Biochimie 77*, 631−642.
36. Choong, Y. S., and Massey, V. (1980) Stabilization of lactate oxidase flavin anion radical by complex formation, *J. Biol. Chem. 255*, 8672−8677.
37. Tegoni, M., and Cambillau, C. (1994) The 2.6 Å refined structure of the *Escherichia coli* recombinant *Saccharomyces cerevisiae* flavocytochrome $b_2$-sulfite complex, *Protein Sci. 3*, 303−313.
38. Tegoni, M., Begotti, S., and Cambillau, C. (1995) X-ray structure of two complexes of the Y143F flavocytochrome $b_2$ mutant crystallized in the presence of lactate or phenyllactate, *Biochemistry 34*, 9840−9850.
39. Mowat, C. G., Beaudoin, I., Durley, R. C., Barton, J. D., Pike, A. D., Chen, Z. W., Reid, G. A., Chapman, S. K., Mathews, F. S., and Lederer, F. (2000) Kinetic and crystallographic studies on the active site Arg289Lys mutant of flavocytochrome $b_2$ (yeast L-lactate dehydrogenase), *Biochemistry 39*, 3266−3275.
40. Labeyrie, F., Beloeil, J. C., and Thomas, M. A. (1988) Evidence by NMR for mobility of the cytochrome domain within flavocytochrome $b_2$, *Biochim. Biophys. Acta 953*, 134−141.
41. Gao, Y. T., Smith, S. M., Weinberg, J. B., Montgomery, H. J., Newman, E., Guillemette, J. G., Ghosh, D. K., Roman, L. J., Martasek, P., and Salerno, J. C. (2004) Thermodynamics of oxidation−reduction reactions in mammalian nitric-oxide synthase isoforms, *J. Biol. Chem. 279*, 18759−18766.
42. Hazzard, J. T., McDonough, C. A., and Tollin, G. (1994) Intramolecular electron transfer in yeast flavocytochrome $b_2$ upon one-electron photooxidation of the fully reduced enzyme: evidence for redox state control of heme-flavin communication, *Biochemistry 33*, 13445−13454.
43. Walker, M. C., and Tollin, G. (1991) Laser flash photolysis studies of the kinetics of electron-transfer reactions of *Saccharomyces* flavocytochrome $b_2$: evidence for conformational gating of intramolecular electron transfer induced by pyruvate binding, *Biochemistry 30*, 5546−5555.
44. Walker, M. C., and Tollin, G. (1992) Laser flash photolysis study of the kinetics of electron-transfer reactions of flavocytochrome $b_2$ from *Hansenula anomala*: further evidence for intramolecular electron-transfer mediated by ligand binding, *Biochemistry 31*, 2798−2805.
45. Lê, K. H. D., and Lederer, F. (1991) Amino acid sequence of long chain α-hydroxy acid oxidase from rat kidney, a member of the family of FMN-dependent α-hydroxy acid-oxidizing enzymes, *J. Biol. Chem. 266*, 20877−20981.
46. Schuman, M., and Massey, V. (1971) Effect of anions on the catalytic activity of pig liver glycolic acid oxidase, *Biochim. Biophys. Acta 227*, 521−537.
47. Schuman, M., and Massey, V. (1971) Purification and characterization of glycolic acid oxidase from pig liver, *Biochim. Biophys. Acta 227*, 500−520.
48. Cunane, L. M., Barton, J. D., Chen, Z.-w., Lê, K. H. D., Amar, D., Lederer, F., and Mathews, F. S. (2005) Crystal structure analysis of recombinant rat kidney long-chain α-hydroxy acid oxidase, *Biochemistry 44*, 1521−1531.
49. Sukumar, N., Dewanti, A. R., Mitra, B., and Mathews, F. S. (2004) High-resolution structures of an oxidized and reduced flavoprotein. The water switch in a soluble form of (S)-mandelate dehydrogenase, *J. Biol. Chem. 279*, 3749−3757.
50. Roussel, A., and Cambillau, C. (1989) in *Silicon graphics geometry partner directory*, Silicon Graphics, Mountain View, CA.

BI602634Y